

A simple theory of the pycnocline and overturning- revisited

Anand Gnanadesikan

NOAA Geophysical Fluid Dynamics Laboratory, Princeton, New Jersey.

Agatha de Boer

School of Environmental Science, University of East Anglia, Norwich, United Kingdom.

Bryan K. Mignone

The Brookings Institution, Washington, District of Columbia.

A simple theory linking the pycnocline depth and volume transport of the thermohaline overturning to winds, eddies, surface densities and diapycnal diffusion was proposed by Gnanadesikan (Science, 283:2077-2079, 1999). This paper revisits this theory, with eye to understanding which predictions are robust, and which may be limited by the geometric simplification required to derive such a simple theory. We show that the theory works extremely well for diagnostic models, in which surface density is fixed. It thus appears that the model can be used as a diagnostic framework for understanding mechanisms behind circulation changes. The key insight of the theory that the Southern Ocean, rather than the tropics, can serve as a pathway for transformation of dense water to light water is supported by the observed distribution of radiocarbon. However, we demonstrate that changes in forcing do more than simply scale the magnitude of the circulation up and down, producing changes in pycnocline shape and circulation geometry. In particular, the roles of buoyancy forcing and stationary eddies are more complicated than would be expected from the simple theory. Such changes must be taken into account when interpreting measurements at individual locations.

1. INTRODUCTION

Understanding variability in the meridional overturning circulation requires linking changes in surface forcing and internal mixing to modifications of the thermal structure, differences in the rate of formation of deep waters, and shifts in the locations where these waters are formed. It is thus closely linked to the question of how the ocean circulation is “driven”- which has been debated for many years. In his classic “Physical Geography of the Oceans” (reprinted in 1963), Matthew Fontaine Maury argued that the dominant mechanism for driving such currents was the heating of the tropics and cooling of polar latitudes. In such a picture, one would primarily look to changes in the hydrological cycle or surface heat balance to explain changes in overturning, as in the classic box models of Stommel (1961). By contrast, Maury fulminated against those who supposed that the ocean circulation was wind-driven, arguing that the variable winds of the Atlantic could never produce the steady Gulf Stream.

The idea of a thermally-driven overturning was challenged by Sandstrom (1908) who argued that in a domain where heating occurs at the same level as cooling, a large-scale circulation cannot be generated in the absence of diffusion. While various parts of “Sandstrom’s theorem” appear to be incorrect (Coman et al., 2006), his work contains a fundamental insight. When buoyancy is added at the same level at which it is removed, the vertical buoyancy flux, and hence the buoyancy work is zero (Papparella and Young, 2002; Gnanadesikan et al., 2005). Thus even insofar as the ocean overturning is affected by buoyancy forcing, some source of energy is required to provide the mechanical driving for the system- particularly over long time periods and relatively large vertical length scales (Munk and Wunsch, 1998; Huang, 1999).

Two such sources have been proposed. One is the internal mixing driven by breaking internal waves. In a seminal paper, Bryan (1987) discussed the dynamics of an overturning whose magnitude is controlled by the vertical diffusion- which in turn is governed by the internal wave field controlled by winds and tides. The second possible source of energy is the work done by the wind on the surface geostrophic currents. There are two types of circulation schemes that make use of this idea. The first (most clearly expressed by Toggweiler and Samuels, 1993, 1998) suggests that it is the winds within the Southern Ocean that are most important. Within this scheme, the dominant location where water is transformed from dense to light is the Southern Ocean and changes in the density in the north would be expected to change only the pycnocline depth. A second set of schemes, as described by Salmon (1990), Samelson and Vallis (1997) and Vallis (2000) link the depth of the pycnocline to mid-latitude Ekman pumping. In these schemes the balance is between the wind stress curl- which pumps light water down into the interior, and boundary currents which return it to higher latitudes.

Gnanadesikan (1999, henceforth G99) developed a simple theory that melded the Bryan (1987) and Toggweiler and Samuels (1993) ideas for determining the depth of the pycnocline as well as including the impact of mesoscale eddies. This paper revisits the G99 theory, reviewing some of the ways in which it succeeds in describing ocean models- and some ways in which it falls short. Section 3 demonstrates that the theory works well in a diagnostic sense to explain the overall circulation and that the distribution of radiocarbon supports the idea that the Southern Ocean is in fact the principal region of dense-to-light water conversion in the present-day ocean. However, in the following sections we demonstrate that theory does not capture some aspects of the circulation that are important in interpreting past measurements. Section 4 examines how the geometry of the circulation changes in response to changes in forcing, highlighting the role of stationary eddies. Section 5 discusses the role of the reduced gravity in setting the ge-

ometry and sensitivity of the solutions. Finally Section 6 shows that the shape of the pycnocline may change in response to forcing changes. Section 7 concludes the paper.

2. THEORY AND MODELS

The basic idea behind the G99 theory is illustrated in Figure 1. Closures for the northern overturning M_n and tropical upwelling flux M_u in terms of the pycnocline depth D , which is defined as the depth above which ~80-90% of the density anomaly is found. For purposes of this paper we will adopt the definition

$$D = 2 \frac{\int_{z=-2500}^0 (\sigma_2(z) - \sigma_2(z = 2500)) dz}{\int_{z=-2500}^0 (\sigma_2(z) - \sigma_2(z = 2500)) dz} \quad (1)$$

A depth of 2500m is used to avoid spurious effects due to topography as most of the ocean ridges (at least in the coarse models we use here) lie below these depths. When calculated from the World Ocean Atlas for the region from 30°S to 40°N, D has a value of 894m. Closures to link D with the overturning fluxes may be taken following Bryan (1987) and Park (1999) as

$$M_n = g' D^2 / \varepsilon \quad (2a)$$

$$M_u = 2K_v A / D \quad (2b)$$

Where g' is the density contrast associated with the pressure gradient driving the overturning, ε is a “resistance coefficient” which embodies the effects of friction and geometry, K_v is the vertical diffusive coefficient, and A is the area of the tropical oceans. G99 added two other terms in the Southern Ocean, an Ekman upwelling term M_{ek} and an eddy-induced advection term M_{eddy} .

$$M_{ek} = \tau L_x / \rho f \quad (3a)$$

$$M_{eddy} = A_I L_x D / L_y \quad (3b)$$

Where τ is the mean wind stress at the tip of Drake Passage, L_x is length of the latitude circle, ρ is the density, f the Coriolis parameter, A_I the Gent-McWilliams diffusion coefficient and L_y the horizontal scale over which the pycnocline shallows in the south. Assuming a steady-state mass balance then leads to

$$g'D^2 / \varepsilon + A_l L_x D / L_y = \tau L_x / \rho f + 2K_v A / D \quad (4)$$

This equation has several revealing limiting cases. If the Southern Ocean terms are set to zero, one recovers the result of Bryan (1987) that the overturning

$$D = (2K_v A \varepsilon / g')^{1/3} \quad (5a)$$

$$M_n = M_u = (g' K_v^2 A^2 / \varepsilon)^{1/3} \quad (5b)$$

This classic result suggests that increasing the density contrast between the polar North Atlantic and the tropics will result in reducing the pycnocline, but increasing the overturning. It also requires a relatively large vertical diffusion to supply the roughly 18 Sv of NADW formation. If A is the area of the oceans between 30°S and 40°N ($2.0 \times 10^{14} \text{ m}^2$) and $D=894\text{m}$, then the required diffusion is $4 \times 10^5 \text{ m}^2/\text{s}$. Following recent calculations by St. Laurent and Simmons (2006) the energy required to support such a high mixing coefficient is 2.2 PW for the pycnocline alone, far larger than the approximately 1 PW supplied by winds. A key prediction of this model is thus that tidal mixing should play a major role in overturning and climate. A second prediction which is relevant to paleoclimate is that changes in the hydrological cycle will produce opposite changes in the pycnocline depth and overturning. The only way to get the both the overturning and pycnocline depth to decrease (as for example Lynch-Stieglitz et al., 1999 suggest occurred during the last Ice Age) is to decrease the diapycnal diffusion coefficient.

A second limit of the theory is when K_v is set to 0 and, as in Marshall and Radko (2003), the vertical diffusion coefficient depends on the slope of the pycnocline ($A \sim D$). In this limit the pycnocline depth goes as the square root of the wind stress, with the fraction of upwelling supplied by diapycnal transformation or transient eddy fluxes remaining constant. This limit qualitatively describes eddy-resolving models of the Southern Ocean (Hallberg and Gnanadesikan, 2001,2006) in cases where the Ekman flux is not significantly larger than the buoyancy transformation. In this version of the theory, both pycnocline depth and overturning can decrease if the Southern Ocean winds decrease and the pycnocline depth goes as the square root of the wind stress.

It has been noted that the G99 theory does not include a representation of the effects of mid-latitude wind stress curl. One reason for this may be found in the contemporaneous simulations reported in Gnanadesikan and Hallberg (2000) that look at the impact of changes in wind stress and wind stress curl on the transport of the Antarctic Circumpolar Current. In this work, wind stress offsets that changed the Ekman flux, but not the Ekman pumping were compared with increases and decreases in the magnitude of

the wind stress. As seen in Figures 10 and 14 of Gnanadesikan and Hallberg (2000), the runs with offsets are not significantly different from the runs with winds scaled up and down, suggesting that it is the stress and not the wind stress curl that matters (at least in diagnostic models).

There have been a number of tests of the theory in addition to the qualitative evaluation of G99. One particular area of concern has been the degree to which the northern overturning and density structure responds to Southern Ocean winds. Klinger et al. (2003) demonstrated that the G99 theory worked in a set of idealized ocean-only models, but argued that the wind effect was relatively small. Vallis (2000) also found a relatively small effect from changing Southern Ocean winds but a noticeable impact of changing the low-latitude wind stress curl. Gnanadesikan et al. (2003) presented an evaluation of the theory for a relatively limited set of coarse-resolution global runs arguing that dominance of tropical upwelling seen in Klinger et al. (2003) and Vallis (2000) was a result of using a small basin. This study did not, however, look at how well the theory predicted the response to changes in winds.

A second area of concern regards the role of density (subsumed in the g' parameter), which may be more complicated than allowed for in the G99 theory. In general, the buoyancy flux Q must simply balance the cross-density transport $V\partial B/\partial y$. In diagnostic runs the surface buoyancy field B is fixed and so the buoyancy flux is tightly linked to changes in wind stress that change the surface velocity V . While such a linkage may be realistic for temperature it is unlikely to be realistic for salinity. It is therefore suggestive that a number of other experiments in which the surface density is more free to vary the response of the overturning to changes in Southern Ocean winds (Rahmsdorf and England, 1997), vertical diffusion (Mignot et al., 2006) or isopycnal diffusion (Griesel and Maqueda, 2006) do not necessarily agree with the G99 theory. We will examine this issue in more detail.

We now have available to us two new sets of models. One set explores the range of parameters in much greater detail than in G99 and Gnanadesikan et al. (2003) while retaining the restoring surface boundary conditions used in G99. The other examines the effect of relaxing the strong restoring (particularly of salinity).

The first set of runs consists of a suite of 17 ocean-only simulations in a realistic geometry at a nominal resolution of 4 degrees with 24 vertical levels, described in Gnanadesikan et al. (2002), Mignone et al. (2006) and Mignone (2006). In these models, climatological monthly fluxes of heat and salt are applied to the surface and flux corrections are computed by restoring the surface temperature and salinities towards observations with a 30 day time scale. The wind stress, vertical diffusion coefficient in the upper water column, and lateral diffusion coefficient are varied together so as to produce similar pycnocline depths according to the

G99 theory, and separately to isolate the individual effects of each process. The parameters varied are the vertical diffusion, lateral diffusion and wind stress. Values for the vertical diffusive coefficient in the upper 1000m range from $0.15 \text{ cm}^2/\text{s}$ (essentially making the assumption that the measurements of Ledwell et al., 1993 are representative for the pycnocline as a whole) to $1.2 \text{ cm}^2/\text{s}$. Values for the lateral diffusive coefficient A_l range from $100 \text{ m}^2/\text{s}$ to $6000 \text{ m}^2/\text{s}$. The parameter settings are given in columns 2-4 of Table 1. In addition to the model physics, the abiotic carbon cycle was simulated in all of these runs including the effects of bomb radiocarbon using the Ocean Carbon Model Intercomparison Project, Version 2 protocols (Watson et al. 2003). This enables us to compare the simulations produced by these solutions with observations of radiocarbon.

A second set of runs for which surface buoyancies are allowed to vary is made in an idealized two-basin configuration, following the work of De Boer et al. (2007a,b). This model consists of a coarse-resolution (4 degree) ocean model coupled to a dynamic sea ice model and an energy-moisture balance atmosphere. The ocean model topography is highly idealized, with a “Pacific-Indian” basin twice the size of a narrower “Atlantic” basin, and a set of ridges distributed throughout the ocean to represent the effect of mid-ocean ridges. The vertical diffusion in this model is similar to the low-mixing values in the diagnostic suite, varying from $0.1 \text{ cm}^2/\text{s}$ in the pycnocline to $1.2 \text{ cm}^2/\text{s}$ at the ocean bottom and the lateral diffusion coefficient (used for both the GM eddy bolus flux and isopycnal diffusion) is set to $800 \text{ m}^2/\text{s}$. Surface wind stresses are given by the zonal component of the ECMWF wind stresses. In terms of the mechanical forcing, the simple coupled model is thus closest to model 7 in the diagnostic suite.

Surface buoyancy fluxes are given by a one-layer energy balance model whose prognostic variables are temperature and mixing ratio. The temperature depends on the balance between radiation fluxes at the top and bottom of the domain, lateral diffusion, and latent heat released when precipitation is formed. The mixing ratio depends on evaporation from the ocean, precipitation and lateral diffusion. When it exceeds the temperature-dependent saturation mixing ratio, water vapor condenses. Precipitation that falls on land runs off to the nearest ocean point. De Boer et al. (2007a,b) report a large number of simulations with this configuration. We present a subset of these runs in which the wind stress in the Southern Ocean is multiplied by a factor ranging from 0-3.

3. THE G99 THEORY IN AN OCEAN-ONLY MODEL

We begin by examining how the theory describes the behavior of the suite of ocean-only models. We identify M_n as the net northward transport of water with a potential

density σ_0 less than 27.4 at a latitude of 40°N and M_s as the net northward transport of water with a potential density σ_0 less than 27.4 at a latitude of 30°S. D is averaged over the latitude range 30°S to 40°N. Columns 4-7 in Table 1 show the modeled D and M_s , M_n , and $M_u = M_n - M_s$. By inspection, it is easy to see that the G99 theory reproduces the qualitative sensitivity of the simulations to changes in subgridscale parameters. Increasing the Southern Ocean winds increases M_s and M_n . Increasing the A_I coefficient causes M_s to become more negative and M_n to decrease. Increasing K_v causes more upwelling in the tropics, makes M_s more negative and M_n larger.

A more quantitative comparison is given in Figure 2, where the results of the model suite are compared with the G99 theory. We begin with a version in which the relevant parameters are estimated from data. As above, A is the area of the oceans between 30°S and 40°N ($2.0 \times 10^{14} \text{ m}^2$) and we assume that the observed $D=894\text{m}$ is associated with 18 Sv of overturning in the North Atlantic (as for example in Talley et al., 2003) giving us a value for $g'/\epsilon=22.5$. Additionally, we let $L_x=2.5 \times 10^7 \text{ m}$ and $L_y=1.2 \times 10^6 \text{ m}$. Despite not being tuned to the models the variation predicted by the theory is highly correlated with the model output, accounting for at least 90% of the variation in D , M_s , M_u , and M_n . There are however, systematic differences between the theoretical and modeled results, with the predicted D showing significantly less range than the models, and the transports in general being overestimated.

It is possible to estimate the parameters in (5) from the model, individually regressing the overturning flux against D^2 , the tropical upwelling flux against K_v/D and the southern upwelling flux against the Ekman flux at 50S and $A_I D$. When this is done, one obtains the solutions shown by the circles in Figure 2, which have a mean absolute error of 74 m for the pycnocline depth (vs. 105 for the nonoptimized model), and less than 2 Sv for each of the transports. The optimized model has a much smaller apparent area for the upwelling ($1.13 \times 10^{14} \text{ m}^2$). This implies that within these realistic models a very high diffusion coefficient would actually be required to get most of the upwelling occurring in the tropics. The regression also predicts that only about half of the Ekman flux at 50°S actually results in a transformation of dense water to light water at 30°S. We will discuss the reasons for this in Section 4.

These results support the idea of Toggweiler and Samuels (1993) and G99 that the global overturning *can* be driven by the Southern Ocean wind, and demonstrate that the necessary condition for this is that the winds are sufficiently high and the vertical diffusion sufficiently low. They do not, however prove that it *must* be driven by the winds. An additional tracer that has been used to examine this question is radiocarbon. Produced by cosmic rays in the atmosphere- most radiocarbon is taken up by ocean

waters, decaying over time. As discussed in Toggweiler and Samuels (1993) models with excessive upwelling in the low latitudes tend to have excessively low values of radiocarbon. Gnanadesikan et al (2004) showed that this was true for a subset of the models used here (lines 5, 9, 15, and 16 in Table 1) and suggested that such models would also have values of Southern Ocean radiocarbon that were significantly too high. The new model suite gives us an opportunity to extend this result. Figure 3 shows a plot of the mean tropical and Southern Ocean surface radiocarbon plotted against the ratio of tropical upwelling to northern hemisphere overturning. When this ratio is high, the overturning is driven by mixing, when it is low, it is driven by Southern Ocean winds. The observed values are taken from the WOCE survey (Key et al., 2004) corrected to a date of 1990 by adding 20 per mille to match the model changes between 1995 and 1990. The data shows relatively high values in the tropics and very low values in the Southern Ocean. As the models enter regimes where a substantial fraction of the northern hemisphere overturning is supplied by tropical upwelling they are not able to capture either the observed values or the difference between the tropics and high latitudes. Thus, while it is possible to match the observed pycnocline depth and many aspects of the flow field with high vertical and horizontal diffusion, this solution is unlikely to actually describe the real ocean at present.

Taken together, the diagnostic models support the key insight of the G99 theory, namely that high vertical diffusion is not needed to drive the global meridional overturning circulation and that the lightening of deep water in the Southern Ocean is the dominant pathway by which dense abyssal waters are converted to light surface waters. Moreover it appears that the model is quantitatively useful as well, predicting the magnitude of differences between models that result from changing the subgrid-scale parameters. For a simple model, these are significant accomplishments. However, it is worth examining the limits of the theory as well as its successes, and we will focus on some such limits in the following sections.

4. CHANGES IN FLOW PATHWAYS

A particular limitation of the theory is that it does not specifically distinguish between the Pacific, Atlantic and Indian Oceans. This leads to a number of questions. In particular, do changes in one basin really propagate through to other basins? Is the sensitivity to wind driving uniform across basins, or is there more structure involved? We can use the diagnostic model suite to address these questions as well. We focus on the light water (σ_0 lighter than 27.4) transport through 8 sections: 1. the South Pacific at 30°S 2. the Indonesian throughflow 3. the South Indian at 30°S 4. the Indian Sector of the Antarctic (30°E to 140°E at 40°S- which in this model intersects the Australian continent). 5. the Atlantic Sector of the Southern Ocean at 40°S (60°W to

30°E), 6. the flow between the Indian and Atlantic Oceans at 30°E north of 40°S 7. the flow in the Atlantic Ocean at 30°S and 8. the flow in the Atlantic Ocean at 40°N. Figure 4a shows these flows in subset of models (lines 5,12,14 and 16 in Table 1) corresponding to vertical diffusion coefficients of 0.15, 0.3, 0.6 and 1.2 cm²/s. and Figure 4b shows a second subset (corresponding to lines 5, 13, 15 and 17) where the isopycnal diffusion coefficient is altered to match these vertical diffusion coefficients. Figure 5 does the same for the wind stress and lateral diffusion coefficients. A number of important conclusions can be drawn from these plots.

First, we notice that many of the pathways are relatively constant. All the models show a net northward flow of light water in the South Pacific, flow through the Indonesian archipelago and a net *southward* flow of light water if one adds up the Atlantic and Indian Ocean. The relative magnitude of these pathways does not change substantially if one varies only the vertical diffusion coefficient (Figure 4a). The majority of the flow in the circulations where K_v is varied enters the Atlantic from the south (the classic “cold water pathway”, not from the Indian ocean (the classic “warm water pathway”).

Second, there are substantial variations in whether the light waters in the Atlantic at 30°S are fed by northward flow in the Atlantic at 40°S or by flow around the Agulhas. Increasing the winds increases the warm water pathway-actually driving the net light water flow negative in the Atlantic sector. This suggests that, at least in the coarse GCMs, the Atlantic inflow is not strictly controlled by Atlantic winds (a la Nof, 2003) so that the G99 picture is in fact reflecting a global circulation, not one limited to a single basin. Increasing the isopycnal diffusion coefficient has the reverse effect- favoring an inflow in the Atlantic Sector, and in some cases actually reversing the flow in across 30°E in the Agulhas region.

Third, none of these models show a classic “conveyor belt” as outlined by Broecker (1991) in which deep waters (in particular NADW) upwell in the Indian and Pacific Ocean, move through the Indonesian throughflow and are carried around the tip of Africa into the Atlantic. The return flow of NADW in all of the models primarily passes through the Southern Ocean at some point. In the high diffusion models (Figure 4b) the bulk of the return flow upwelling in the Pacific feeds into the Antarctic Circumpolar Current and thence around South America in the cold water pathway. In the low-diffusion, high wind models, the dominant upwelling occurs in the Southern Ocean rather than in Central Pacific, though one can then trace the path of light water from the Pacific, through the Indonesian throughflow, around the Agulhas and on into the Atlantic.

Fourth, the model suite demonstrates that isopycnal diffusion plays a very significant role in determining whether the return flow enters the Atlantic in the warm water or

cold water pathway. This can be seen by comparing the compensated models (which all show relatively weak flow around the Agulhas) with the uncompensated models. The interplay between flow in the Agulhas, South Atlantic sector of the ACC and Indian Ocean sector of the ACC reveals that the southward flow of water associated with increasing eddy diffusion is not simply diffusive. Increasing the eddy diffusive coefficient actually *increases* the net northward flow of light water in the Atlantic sector of the ACC (compare 5a and 5b), something that makes very little sense in the context of a purely diffusive circulation.

The reason for this is that the “eddy” flow is not, in fact, purely diffusive. Hallberg and Gnanadesikan (2001) discuss the three ways in which the northward Ekman transport within Antarctic latitudes can be returned to the South. The first involves deep flow below the ridges and water-mass transformation to the north and south of the ACC, i.e. the meridional overturning circulation. The second is the bolus flux associated with transient eddies. The third involves stationary eddies. Many theories of the ACC assume that the buoyancy transport associated with stationary eddies is essentially zero (for example Marshall and Radko, 2003) and observational studies such as Sun and Watts (2002) which assume a spatially and temporally uniform level of no motion appear to support this idea- predicting relatively small heat fluxes. However, this is not necessarily the case in realistic models in which the level of no motion is actually highly variable in space and time. Nor are these fluxes solely associated with the mean flow- Hallberg and Gnanadesikan (2006), for example, find that highly localized eddy fluxes linked to topographic features can feed significant amounts of subtropical water into the Southern Ocean.

The actual changes in the flow of warm water between the two high wind runs (lines 11 and 9 in Table 1) are examined in Figure 6. The dominant feature resulting from reducing the lateral diffusion coefficient is a change in the transport of light water within the ACC. This change is reflected in a deepening of the light water layer. The changes in the flow into the Indian and Atlantic basins represent relatively small changes in this flow, and are clearly associated with topographic features. This is one important reason that the optimized coefficients for the overturning involve a much weaker dependence on isopycnal diffusion and wind stress than would be assumed from looking at the data. Stationary eddies actually play an important role as well, in ways that have yet to be properly explored.

5. THE ROLE OF DENSITY

We have seen that changes in wind and transient eddies can lead to changes in the flow geometry. These changes may be even more extreme when density is allowed to vary as well. This phenomenon is illustrated in Figure 7, which

shows results from the suite of simple coupled models under changing winds. The figure shows the age at a depth of 1600m as the winds increase. For no winds, young water is only found in the northern part of the narrower “Atlantic” basin. As the winds increase, convection begins to occur in the Southern Ocean and wider basin, which is an analog for the Pacific as well. Such a change of geometry is outside the bounds of the G99 theory, though as shown below, the theory can be deployed to help explain how the phenomenon works.

One prediction of the theory, that increasing winds will result in increasing overturning is qualitatively borne out (Figure 8a). The northward flow of light waters at 40°N does increase with the wind, both globally and in the narrower basin which is an analog for the Atlantic. Additionally, the prediction that the pycnocline depth should increase as the wind increases is also borne out (Figure 8b). Additionally, as suggested by the theory there is a switch (not shown) from the primary supply of this light water occurring in the tropics at low winds to being dominated by the Southern Ocean at high winds.

The details of the dependence however, are surprising. The overturning in the Pacific increases much more strongly than in the Atlantic. Tripling the wind stress from a factor of 1 to 3 results in an increase of the Atlantic overturning from 20 Sv to 28 Sv- implying that the Pacific overturning goes from -2 to 26 Sv. Based on the diagnostic models we would not expect such a large increase in the Pacific, as it would be expected that a deepening in the pycnocline would result in more eddy flux to the south.

De Boer et al. (2007a) discuss this phenomenon in terms of the salinity balance between the deep and surface ocean. The winds in the Southern Ocean upwell water that is saltier on average than the salinity of newly formed North Pacific Deep Water. Thus an increase in upwelling will tend to make the surface ocean saltier. When the surface ocean becomes sufficiently salty the North Pacific halocline breaks down, allowing dense water to form there as well, a process which is the reverse of the classic mixed boundary condition thermohaline catastrophe (Stommel, 1961). This phenomenon is reflected in the fact that the density anomaly decreases as the wind stress increases (Figure 8c).

However, in order for the theory to be truly predictive, parameters such as ε , the resistance parameter between the integrated pressure difference $g'D^2$ and the overturning M_n should be constant. As can be seen in Figure 8d, this is not the case when the global overturning and pycnocline depth are used. However, when just the Atlantic is examined, the scaling parameter is relatively constant, and the scaling parameter at high winds is approximately one half that of that for the single basin (as would be expected if there were two identical “drains” for the flow instead of one). Thus although the theory does not predict when and how the flow switches between these regimes, it does provide a

qualitative description of how this change occurs. Note that an important difference between the models will be the flow of water between basins, which as we indicated in the previous section is not a simple function of subgridscale parameterization.

The sharp changes in flow geometry associated with changing deep water formation regions suggest that there may be another regime as well, where the density in the north is always *lighter* than the density in the South. This is the situation in the model of Vallis (2000). In such cases, we would expect the return flow of light water to be associated with some combination of stationary and transient eddies. Johnson et al. (2007), for example, develop a box model in which the dominant return pathway is through transient eddies. In such a scenario, the pycnocline depth and overturning may have some dependence on wind stress curl as the pycnocline depth will then be determined by a balance between local Ekman pumping and upwelling.

6. THE SINGLE LENGTH-SCALE APPROXIMATION

We have seen that changes in winds, mixing or density do not necessarily affect all locations in the horizontal in the same way. An additional question is how they affect the structure in the vertical- a question particularly relevant to extrapolating paleoclimate data in the vertical. One implicit assumption of the G99 theory is that there is a single length scale that describes the structure of the pycnocline- or in other words that the shape of the density gradient is self-similar across a range of parameter values. It is by no means obvious that this should be true. A number of thermocline theories, for example those of Salmon (1990) and Vallis (2000), distinguish between the *depth* at which the pycnocline is found and the *thickness* of the pycnocline at that depth. We may distinguish between these two concepts by denoting the pycnocline depth D as in (1) while the thickness of the gradient region H is described as

$$H = \frac{(\rho(z=0) - \rho(z=-2.5km))^2}{\int_{z=-2.5km}^0 (\partial\rho/\partial z)^2 dz} \quad (6)$$

This formula gives the correct answer both for a linear and exponential profile. For an exponential profile $D=H$ (twice the e-folding depth), but for other profiles (as illustrated in Figure 9) will not be the case. A linear profile (Figure 9b) will have $H=1.5D$, while for a parabolic profile (not shown) where $\rho=\rho_0-\delta\rho(z/D_0+1)^2$, $H=0.5D$.

The distribution of H and D are noticeably different, both in data (Figure 10a and b) and in models (Figure 10c, d; Table 1). In particular, D has relatively little variation

over the low latitudes, while H becomes very thin in the tropics. In most places, however, H/D lies within the range of 0.5-1.5 that can be associated with profiles characterized by a single length scale. The average H in the data between 30S and 40N is 514m. On the face of things, this would suggest that D and H are not separate scales as suggested in Salmon (1990) and Vallis (2000).

An examination of the dependence of D and H on sub-grid scale parameters (Table 1), however, shows that while the two are similar in terms of magnitude, they have different dependencies. For example, increasing the wind stress increases D (in agreement with the G99 theory) but not H . As seen in Figure 10c and d, it is possible to increase K_v and A_I together to maintain D , but such combinations do not maintain H . This demonstrates clearly that the shape of the thermocline is not in fact constant under different parameter settings- so that one should not expect too much from a theory that assumes geometric similarity. At low values of K_v , H is relatively insensitive to changes in wind stress or Southern Ocean eddies.

It is worth examining the behavior of H when K_v is large. High values of K_v result in noticeably higher values of H in the tropics (ranging over about 150m) and northern hemisphere (with zonal differences approaching 400m), causing H and D to become of comparable magnitudes when a global average is taken. When this is the case, increasing A_I reduces both H and D . Note that the observations do have H significantly smaller than D further supports the assertion that low values of K_v are more consistent with the ocean as we see it today.

7. CONCLUSIONS

We have demonstrated that the theory developed in G99 has significant skill in diagnosing the driving mechanisms for the meridional overturning circulation- providing a number of useful insights for thinking about how the circulation works. First, it provides a framework for demonstrating how internal mixing may be replaced by Southern Ocean wind-driven upwelling as a driving mechanism for the global overturning. This highlights the importance of Southern Ocean winds, a topic dealt with elsewhere in this volume (Saenko, 2007). Second, it points out that the pycnocline provides a connection between the Southern Ocean and North Atlantic (or other deep water formation regions), and that changes in one may result in changes in the other. Third, it emphasizes the importance of the hydrological cycle, not merely in slowing down the overturning by freshening the northern latitudes, but actually maintaining it with respect to the Southern Ocean and by setting locations of sinking.

We have also noted that the G99 theory has some shortcomings related to the simplifications required to derive such a simple closure for the circulation. The biggest of these is that it effectively assumes a constant geometry of both the

flow field and the density structure. This paper shows that changes demonstrates that the shape of the pycnocline in the vertical and the locations of deep water formation in the horizontal can result in behavior that is not intuitive, such as an increase in Southern Ocean winds causing switch in the dominant location of deep water formation between the Atlantic and Pacific, or a decrease in the cold water pathway. Moreover, the fact that a significant fraction of the light water exchange between the Southern Ocean and low latitudes is mediated by stationary eddies- a process not included in the G99 theory- results in the failure of the theory to predict how changing isopycnal diffusion will change the light water flow in various sectors of the Southern Ocean. This final shortcoming however, still highlights the importance of Southern Ocean for the global circulation, suggesting that explanations for long-term changes must consider this region, as well as looking at the deep water formation zones.

Acknowledgments. The authors thank the Geophysical Fluid Dynamics Laboratory for support of this research, Robbie Toggweiler for many useful discussions, and Rick Slater and Joellen Russell for assistance carrying out the calculations. ADB received support from the NSF Earth System History program under grant NSF OCE-0081686 and from the Visiting Scientist Program at GFDL. BKM acknowledges support from BP/Amoco and Ford under the Princeton Carbon Mitigation Initiative. Comments from Helen Johnson, Laura Jackson, and two anonymous reviewers are also gratefully acknowledged.

REFERENCES

- Broecker, W. S., The great ocean conveyor. *Oceanography*, 4, 79-89, 1991.
- Bryan, F., Parameter sensitivity of primitive-equation ocean general circulation models, *J. Phys. Oceanogr.*, 17, 970-985, 1987.
- Coman, M., R.W. Griffiths, and G.O. Hughes, Sandstrom's experiments revisited, *J. Marine Res.*, 64,783-796, 2006.
- De Boer, A. M., D. M. Sigman, J. R. Toggweiler, and J. L. Russell: The effect of global ocean temperature change on deep ocean ventilation. in press *Paleoceanography* 2007a.
- De Boer, A.M., J.R. Toggweiler and D.M. Sigman, Atlantic dominance of the meridional overturning, subm. *J. Phys. Oceanogr.*, 2007b.
- Gent, P., and J. C. McWilliams, Isopycnal mixing in ocean models. *J. Phys. Oceanogr.*, 20, 150-155, 1990.
- Gnanadesikan, A simple theory for the thickness of the oceanic pycnocline, *Science*, 283, 2077-2079, 1999.
- Gnanadesikan, A., J.P. Dunne, R.M. Key, K. Matsumoto, J.L. Sarmiento, R.D. Slater and P.S. Swathi, Ocean ventilation and biogeochemical cycling: Understanding the physical mechanisms that produce realistic distributions of tracers and productivity, *Global Biogeochemical Cyc.*, GB4010, doi:10.1029/2003GB002097, 2004.
- Gnanadesikan, A., and R.W. Hallberg, On the relationship of the Circumpolar Current to Southern Hemisphere winds in large-scale ocean models *J. Phys. Oceanogr.* 30:2013-2034, 2000.
- Gnanadesikan, A., R.D. Slater N. Gruber and J.L. Sarmiento,

- Oceanic vertical exchange and new production: A comparison between models and data , *Deep Sea Res. II* , 49:363-401, 2002.
- Gnanadesikan, A., R.D. Slater and B.L. Samuels, Sensitivity of water mass transformation and heat transport to subgridscale parameterization in ocean general circulation models, *Geophys. Res. Lett.*, 30(18), 1967, 10.1029/2003GL018036, 2003.
- Gnanadesikan, A., R. D. Slater, P. S. Swathi, and G. K. Vallis, The energetics of ocean heat transport. *J. Climate*, 18(14), 2604-2616, 2005.
- Griesel, A., and M.M. Maqueda, The relationship of meridional pressure gradients to North Atlantic Deep Water volume transport in an ocean general circulation model, *Climate Dyn.*, 26, 781-799, 2006.
- Hallberg, R.W. and A. Gnanadesikan, An exploration of the role of transient eddies in determining the transport of a zonally re-entrant current, *J. Phys. Oceanogr.*, 31: 3312-3330, 2001.
- Hallberg, R.W. and A. Gnanadesikan, The role of eddies in determining the structure and response of the wind-driven Southern Hemisphere overturning: Results from the Modeling Eddies in the Southern Ocean Project, *J. Phys. Oceanogr.*, 36 , 2232-2252, 2006.
- Haug, G. H., D. M. Sigman, R. Tiedemann, T. F. Pedersen, and M. Sarnthein, Onset of permanent stratification in the subarctic Pacific Ocean. *Nature*, 401, 779-782, 1999.
- Hellermann, S., and M. Rosenstein: Normal monthly wind stress over the World Ocean with error estimates. *J. Phys. Oceanogr.*, 13, 1093-1107, 1983.
- Huang, R. X., Mixing and energetics of the oceanic thermohaline circulation. *J. Phys. Oceanogr.*, 29, 727-746, 1999.
- Johnson, H.L., D.P. Marshall, and D.A.J. Sproson, Reconciling theories of a mechanically driven meridional overturning circulation with thermohaline forcing and multiple equilibria, in press, *Climate Dynamics*, 2007.
- Key, R.M., and coauthors, A global ocean carbon climatology: Results from GLODAP, *Global Biogeochem. Cyc.*, GB4031, doi: 10.1029/2004GB002247, 2004.
- Klinger, B.A., S. Drijfhout, J. Marotzke and J. Scott, Sensitivity of basin-wide meridional overturning to diapycnal diffusion and remote wind forcing in an idealized Atlantic-Southern Ocean geometry, *J. Phys. Oceanogr.*, 13, 249-266, 2003.
- Lynch-Stieglitz J., W.B. Curry, and N. Slowey, Weaker Gulf Stream in the Florida straits during the last glacial maximum, *Nature*, 402, 644-648, 1999.
- Marshall, J. and T. Radko, Residual-mean solutions for the Antarctic Circumpolar Current and its associated overturning circulation, *J. Phys. Oceanogr.*, 33, 2341-2354, 2003.
- Maury, M.F., The Physical Geography of the Sea and its Meteorology (ed. J. Leighly), Belknap Press, Cambridge, MA., 1963.
- Mignone, B.K., Scientific and political economic constraints on the solution to the global warming problem, Ph.D. Dissertation, Princeton University, 2006.
- Mignone, B.K., A. Gnanadesikan, J.L. Sarmiento and R.D. Slater, Central role of Southern Hemisphere winds and eddies in modulating the ocean uptake of anthropogenic carbon dioxide, *Geophys. Res. Letters* , 33, L01604, 2006.
- Mignot, J., A. Levermann and A. Griesel, A decomposition of the Atlantic Meridional Overturning into physical components using its sensitivity to vertical diffusivity, *J. Phys. Oceanogr.*, 36,

- 636-650, 2006.
- Munk, W. and C. Wunsch, The moon and mixing: Abyssal Recipes II, *Deep Sea Res.*, 45, 1977-2009, 1998.
- Nof, D., The Southern Ocean's grip on the northward meridional flow. *Progress in Oceanography*, 56, 223-247, 2003.
- Paparella, F., and W. R. Young, : Horizontal convection is non-turbulent. *J. Fluid Mech.*, 466, 205-214, 2002.
- Park, Y.-G., The stability of thermohaline circulation in a two-box model, *J. Physical Oceanogr.*, 29, 3101-3110, 1999.
- Rahmstorf, S. and M. H. England,, Influence of Southern Hemisphere winds on North Atlantic Deep Water flow. *Journal of Physical Oceanogr.*, 27, 2040-2054, 1997.
- Russell, J.L., K. W. Dixon, A. Gnanadesikan, R.J. Stouffer and J.R. Toggweiler, Southern Ocean westerlies in a warming world: Keeping open the door to the deep ocean, *J. Climate*, 19, 6381-6390, 2006.
- Saenko, O., Projected strengthening of the Southern Ocean winds: Implications for the deep circulation and mechanical energy budget of the ocean, this volume, 2007.
- St. Laurent, L.C. and H. Simmons, Estimates of power consumed by mixing in the ocean interior, *J. Climate*, 19, 4877-4890, 2006.
- Sandstrom, J.W., Dynamische versuche mit meerwasser, *Ann. Hydrogr. Marit. Meteor.*, 36, 6-23, 1908.
- Salmon, R., The thermocline as an internal boundary layer, *J. Mar. Res.*, 48, 437-469, 1990.
- Samelson, R. M., and G. K. Vallis, Large-scale circulation with small diapycnal diffusion: The two-thermocline limit. *J. Mar. Res.*, 55, 223-275, 1997.
- Stommel, H., Thermohaline convection with 2 stable regimes of flow, *Tellus*, 13, 224-230, 1961.
- Sun C. and D.R. Watts, Heat flux carried by the Antarctic Circumpolar Current mean flow, *J. Geophys. Res.-Oceans*, 107, 3119, doi:10.1029/2001JC001187, 2002.
- Talley, L.D., J.L. Reid and P.E. Robbins, Data-based meridional overturning streamfunctions for the global ocean, *J. Climate*, 16, 3213-3226, 2003.
- Toggweiler, J.R. and B.L. Samuels., Is the magnitude of the deep outflow from the Southern Ocean actually governed by Southern Hemisphere winds?, in *The Global Carbon Cycle*, edited by M. Heimann, pp. 303-331, Springer-Verlag, Berlin, 1993.
- Toggweiler, J. R., and B. L. Samuels, On the ocean's large scale circulation in the limit of no vertical mixing. *J. Phys. Oceanogr.*, 28, 1832-1852, 1998.
- Vallis, G.K., Large scale circulation and production of stratification: effects of wind, geometry and diffusion, *J. Phys. Oceanogr.*, 30, 933-954, 2000.
- Watson, A.J., J.C. Orr and coauthors, Carbon dioxide fluxes in the global ocean, in *Ocean Biogeochemistry: The role of the ocean carbon cycle in climate change*, M.J.R Fasham, ed. Springer-Verlag, pp. 123-144, 2003.

Agatha M. de Boer, School of Environmental Science, University of East Anglia, Norwich, NR4 7TJ, United Kingdom. a.deboer@uea.ac.uk.

Anand Gnanadesikan, NOAA Geophysical Fluid Dynamics Laboratory, PO Box 308, Princeton, NJ 08542, USA Anand.Gnanadesikan@noaa.gov.

Bryan K. Mignone, The Brookings Institution. 1775 Massachu-
setts Ave., NW, Washington, DC 20036, USA.
bmignone@brookings.edu

	K_v	A_I	$\tau(50S)$	D	H	M_s	M_n	M_u
1	0.15	100	1	1126	703	14.2	15.8	1.6
2	0.15	300	0.5	926	677	5.2	9.0	3.8
3	0.15	300	1	1085	711	14.5	15.3	0.8
4	0.15	1000	0.5	818	638	0.5	5.7	5.2
5	0.15	1000	1	920	671	7.1	9.5	2.4
6	0.15	1000	1.02	940	646	6.4	9.4	3.0
7	0.15	1000	1.7	1082	665	15.1	13.9	-1.2
8	0.15	1000	2.5	1202	668	23.3	22.0	-1.3
9	0.15	2000	1	827	638	3.4	6.8	3.4
10	0.15	2000	1.7	970	648	9.2	10.0	0.8
11	0.15	4000	2.5	972	624	10.5	8.7	-1.8
12	0.3	1000	1	962	756	5.3	12.3	7.0
13	0.3	1500	1	926	742	2.8	10.1	7.3
14	0.6	1000	1	1019	867	4.3	17.2	12.9
15	0.6	2000	1	911	801	-4.3	11.8	16.1
16	1.2	1000	1	1086	1036	-1.8	22.9	24.7
17	1.2	6000	1	852	799	-22.3	10.5	32.8

Table 1: Summary of the forcing and overturning in 17 diagnostic coarse-resolution models. Wind stresses at 50S are shown as a multiplier relative to the stress product of Hellermann and Rosenstein.

FIGURE CAPTIONS

Figure 1 : A schematic of the overturning circulation in the G99 model

Figure 2 : Evaluation of the G99 theory compared with a suite of diagnostic models. Nonoptimized results (+) show the G99 model with parameters estimated from data. Optimized results (o) show the G99 model with fluxes individually regressed against their functional form with respect to pycnocline depth D . (a) Pycnocline depth D . (b) NADW formation. (c) Tropical upwelling. (d) Southern Ocean upwelling

Figure 3: Radiocarbon constraints on upwelling pathway. Vertical axis shows surface radiocarbon concentration at a nominal date of 1990 in per mille. Horizontal axis shows the ratio between M_u and M_n , with small values consistent with the Southern Ocean upwelling pathway and large values consistent with tropical upwelling and mixing playing the dominant role. The models are most consistent with very little of the Northern upwelling being supplied through the tropics

Figure 4: Warm water flows across eight sections (positive is eastward/northward, negative westward/southward) for models where vertical diffusion coefficient is varied. Top panel (A) shows models where only K_v is varied. Bottom panel (B) shows models where K_v and A_I are varied so as to compensate for each other (corresponding to the models shown in the bottom panels of Figure 4).

Figure 5: Warm water flows across eight sections (positive is eastward/northward, negative westward/southward) for models where wind stress is varied. Top panel (A) shows models where only wind stress is varied. Bottom panel (B) shows models where

wind stress and A_I are varied so as to compensate for each other.

Figure 6: Illustration of how changing A_I changes the circulation of light water. Plots both show the depth in m of the $s_0=27.4$ surface in colors, and the transport of water above this surface with the vectors. Top: Model with $A_I=4000 \text{ m}^2/\text{s}$ (line 11 in Table 1). Bottom: Model with $A_I=1000 \text{ m}^2/\text{s}$ (line 9 in Table 1).

Figure 7: Age at 1600m (years) from three idealized runs where the winds in the Southern Ocean are scaled up and down. (a) Southern Ocean winds set to 0. Sinking is localized to the “North Atlantic.” (b) Southern Ocean winds at present values. This model produces vertical exchange in the “North Atlantic”, Southern Ocean, and “North Pacific.” (c) Southern Ocean winds increased by a factor of 2 showing expansion of all three deepwater formation regions.

Figure 8: Response of the overturning circulation in a coupled ocean-sea ice-energy moisture balance atmosphere model to changes in Southern Ocean winds. Solid lines show global values, dashed lines those computed for the Atlantic alone. (A) Overturning in Sv. (B) Pycnocline depth in m. (C) Density difference in kg/m^3 . (D) Frictional resistance factor $\epsilon=g'D^2/M_n$.

Figure 9. Schematic of three profiles and the associated values of pycnocline depth (D , eqn 2) and pycnocline thickness (H , eqn. 5) associated with them.

Figure 10: Pycnocline depth and thickness. (a) Pycnocline depth from the 1998 World Ocean Atlas, contours are shown every 400m. b) Pycnocline thickness for the 1998 World Ocean Atlas. c) Zonally averaged pycnocline depth compared with four “compensated” ocean-only models in which horizontal and vertical diffusion are varied together following G99. Note that the lines track each other, and the data, closely. D.) Zonally averaged pycnocline thickness for the same set of models as in c. Note that there is now more variation, with more diffusive models having a notably thicker pycnocline

Figure 1 : A schematic of the overturning circulation in the G99 model.

Figure 2 : Evaluation of the G99 theory compared with a suite of diagnostic models. Nonoptimized results (+) show the G99 model with parameters estimated from data. Optimized results (o) show the G99 model with fluxes individually regressed against their functional form with respect to pycnocline depth D . (a) Pycnocline depth D . (b) NADW formation. (c) Tropical upwelling. (d) Southern Ocean upwelling

Figure 3: Radiocarbon constraints on upwelling pathway. Vertical axis shows surface radiocarbon concentration at a nominal date of 1990 in per mille. Horizontal axis shows the ratio between M_u and M_n , with small values consistent with the Southern Ocean upwelling pathway and large values consistent with tropical upwelling and mixing playing the dominant role. The models are most consistent with very little of the Northern upwelling being supplied through the tropics.

Figure 4: Warm water flows across eight sections (positive is eastward/northward, negative westward/southward) for models where vertical diffusion coefficient is varied. Top panel (A) shows models where only K_v is varied. Bottom panel (B) shows models where K_v and A_I are varied so as to compensate for each other (corresponding to the models shown in the bottom panels of Figure 4).

Figure 5: Warm water flows across eight sections (positive is eastward/northward, negative westward/southward) for models where wind stress is varied. Top panel (A) shows models where only wind stress is varied. Bottom panel (B) shows models where wind stress and A_I are varied so as to compensate for each other.

Figure 6: Illustration of how changing A_I changes the circulation of light water. Plots both show the depth in m of the $\sigma_0=27.4$ surface in colors, and the transport of water above this surface with the vectors. Top: Model with $A_I=4000$ m^2/s (line 11 in Table 1). Bottom: Model with $A_I=1000$ m^2/s (line 9 in Table 1).

Figure 7: Age at 1600m (years) from three idealized runs where the winds in the Southern Ocean are scaled up and down. (a) Southern Ocean winds set to 0. Sinking is localized to the “North Atlantic.” (b) Southern Ocean winds at present values. This model produces vertical exchange in the “North Atlantic”, Southern Ocean, and “North Pacific.” (c) Southern Ocean winds increased by a factor of 2 showing expansion of all three deepwater formation regions.

Figure 8: Response of the overturning circulation in a coupled ocean-sea ice-energy moisture balance atmosphere model to changes in Southern Ocean winds. Solid lines show global values, dashed lines those computed for the Atlantic alone. (A) Overturning in Sv. (B) Pycnocline depth in m. (C) Density difference in kg/m^3 . (D) Frictional resistance factor $\square=g'D^2/M_n$

Figure 9. Schematic of three profiles and the associated values of pycnocline depth (D , eqn 2) and pycnocline thickness (H , eqn. 5) associated with them.

Figure 10: Pycnocline depth and thickness. (a) Pycnocline depth from the 1998 World Ocean Atlas. Contours are shown every 400m. b) Pycnocline thickness for the 1998 World Ocean Atlas. c) Zonally averaged pycnocline depth compared with four “compensated” ocean-only models in which horizontal and vertical diffusion are varied together following G99. Note that the lines track each other, and the data, closely. D.) Zonally averaged pycnocline thickness for the same set of models as in c. Note that there is now more variation, with more diffusive models having a notably thicker pycnocline.

A SIMPLE THEORY OF THE PYCNOCLINE REVISITED

GNANADESIKAN, DE BOER AND MIGNONE

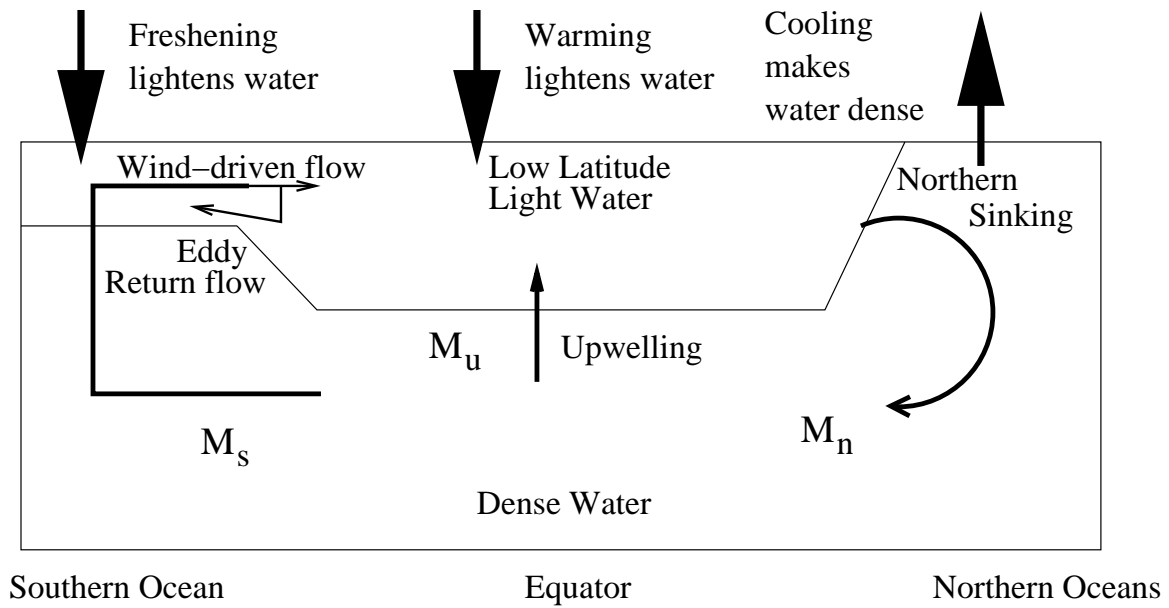


Figure 1 : A schematic of the overturning circulation in the G99 model.

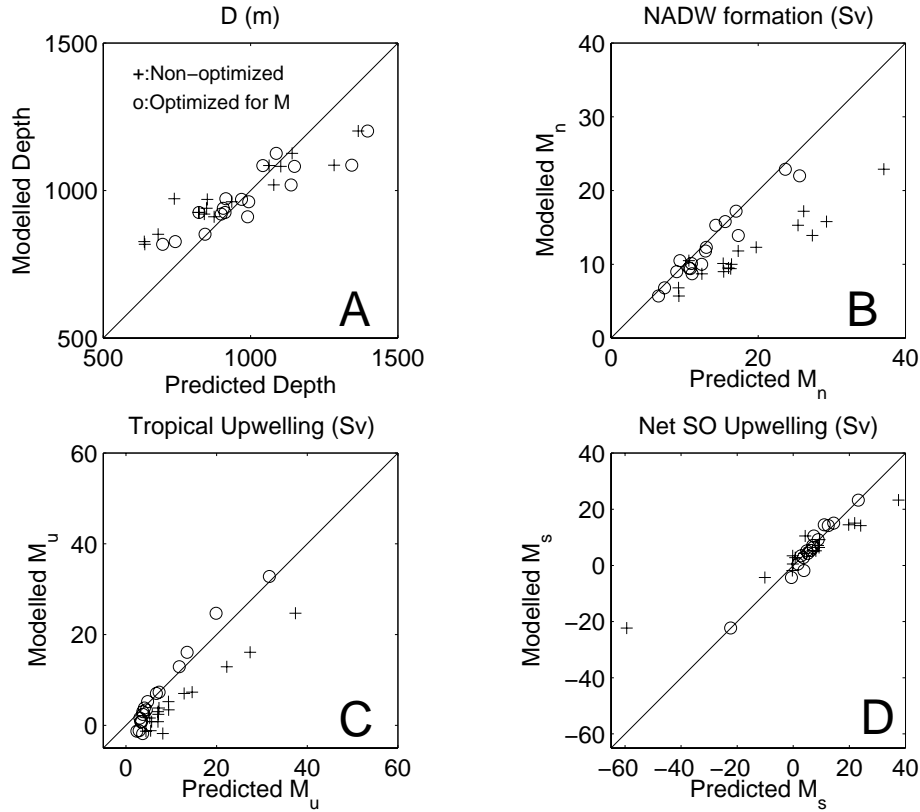


Figure 2 : Evaluation of the G99 theory compared with a suite of diagnostic models. Non-optimized results (+) show the G99 model with parameters estimated from data. Optimized results (o) show the G99 model with fluxes individually regressed against their functional form with respect to pycnocline depth D. (a) Pycnocline depth D. (b) NADW formation. (c) Tropical upwelling. (d) Southern Ocean upwelling.

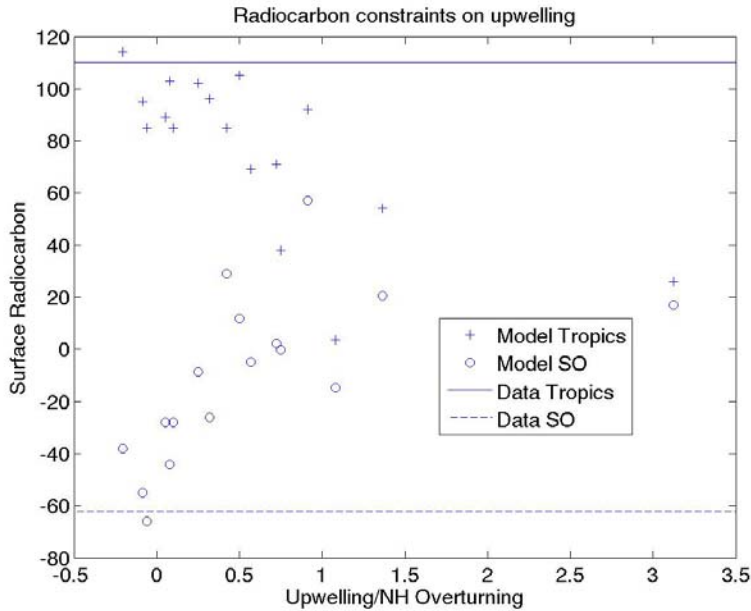


Figure 3: Radiocarbon constraints on upwelling pathway. Vertical axis shows surface radiocarbon concentration at a nominal date of 1990 in per mille. Horizontal axis shows the ratio between M_u and M_n , with small values consistent with the Southern Ocean upwelling pathway and large values consistent with tropical upwelling and mixing playing the dominant role. The models are most consistent with very little of the Northern upwelling being supplied through the tropics.

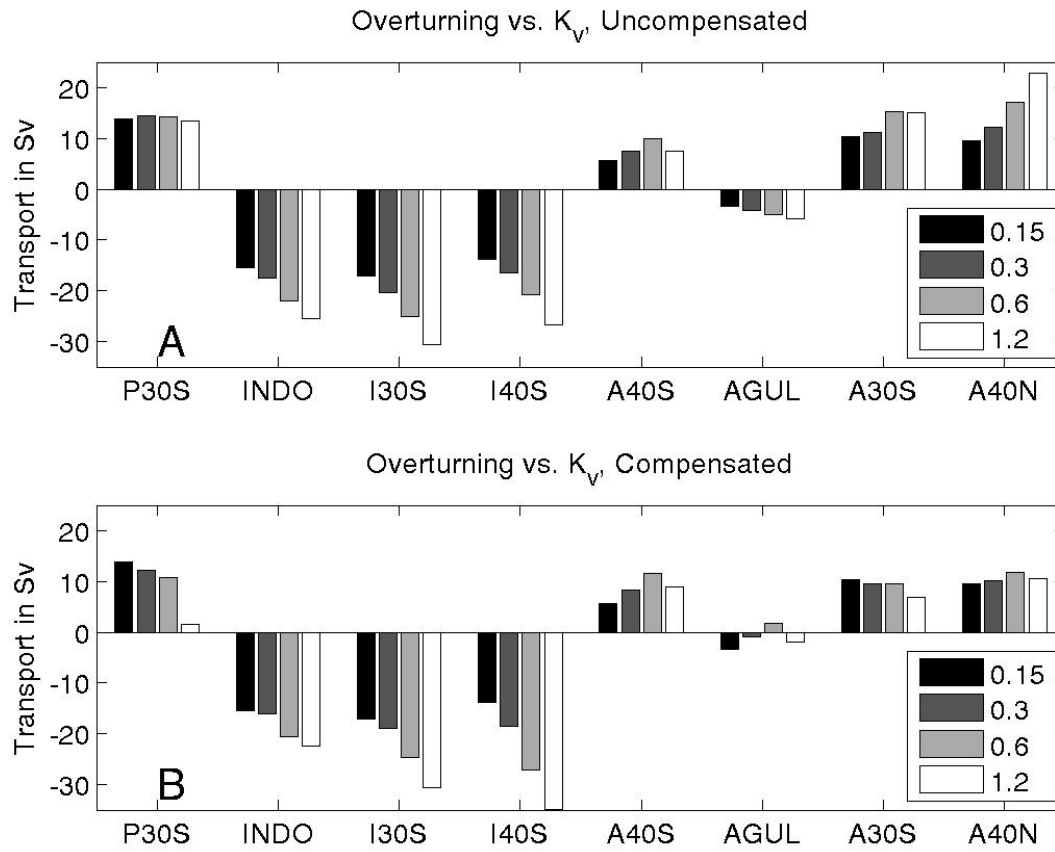


Figure 4: Warm water flows across eight sections (positive is eastward/northward, negative westward/southward) for models where vertical diffusion coefficient is varied. Top panel (A) shows models where only K_v is varied. Bottom panel (B) shows models where K_v and AI are varied so as to compensate for each other (corresponding to the models shown in the bottom panels of Figure 4).

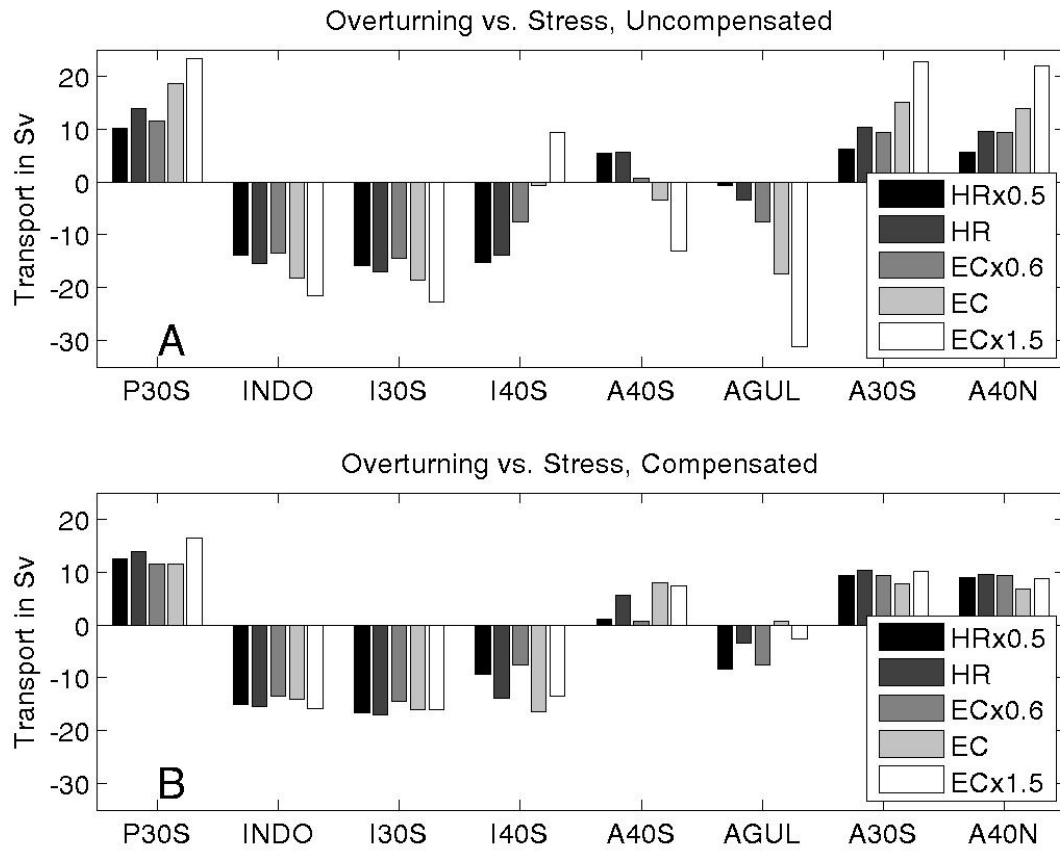


Figure 5: Warm water flows across eight sections (positive is eastward/northward, negative westward/southward) for models where wind stress is varied. Top panel (A) shows models where only wind stress is varied. Bottom panel (B) shows models where wind stress and AI are varied so as to compensate for each other.

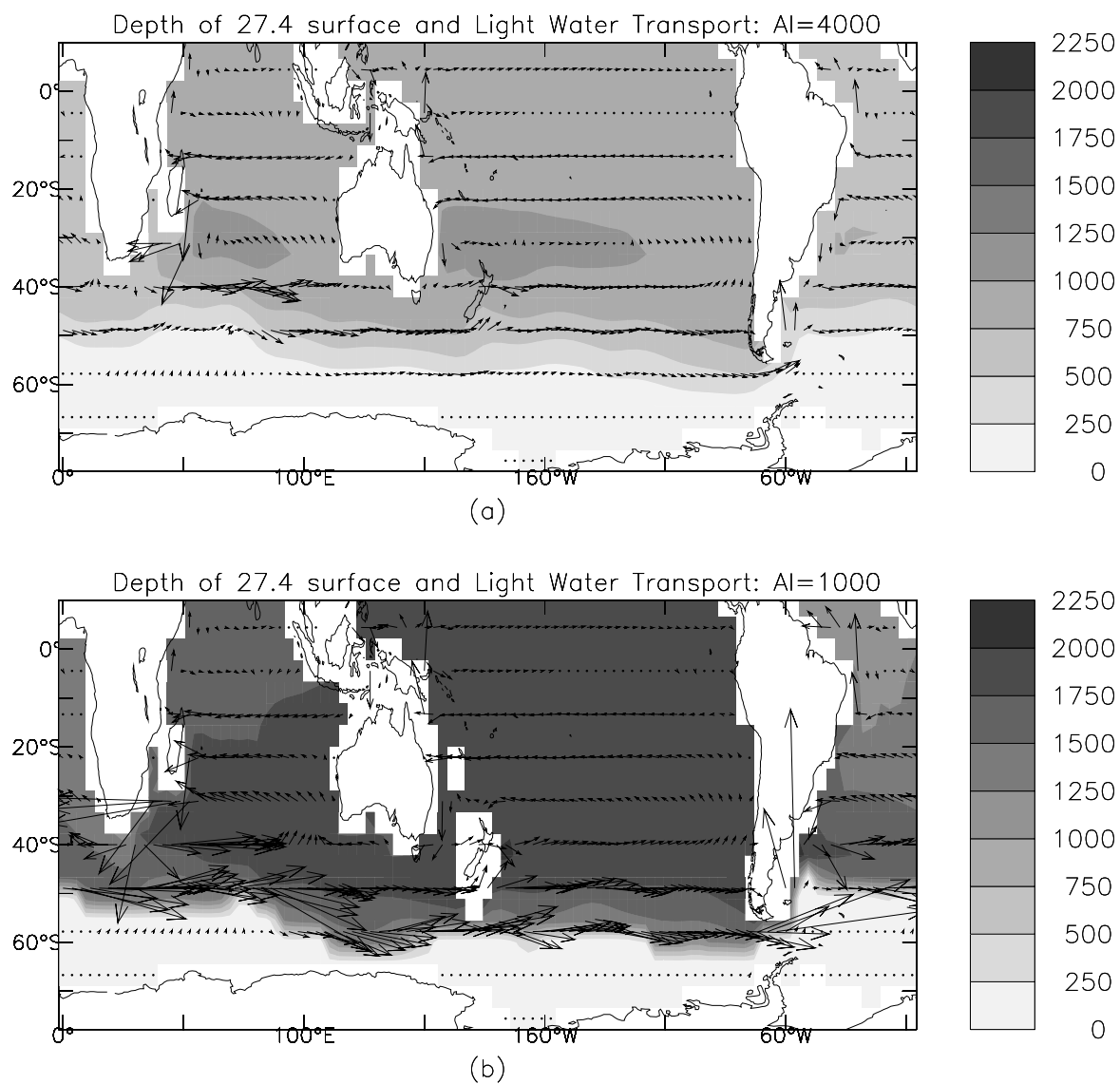


Figure 6: Illustration of how changing A_I changes the circulation of light water. Plots both show the depth in m of the $\sigma_0=27.4$ surface in colors, and the transport of water above this surface with the vectors. Top: Model with $A_I=4000$ m^2/s (line 11 in Table 1). Bottom: Model with $A_I=1000$ m^2/s (line 9 in Table 1).

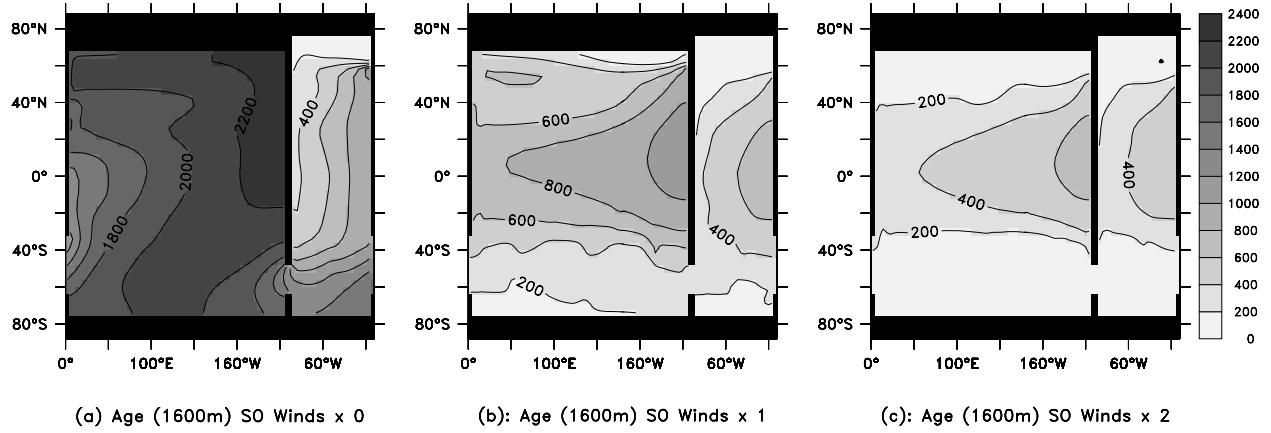


Figure 7: Age at 1600m (years) from three idealized runs where the winds in the Southern Ocean are scaled up and down. (a) Southern Ocean winds set to 0. Sinking is localized to the “North Atlantic.” (b) Southern Ocean winds at present values. This model produces vertical exchange in the “North Atlantic”, Southern Ocean, and “North Pacific.” (c) Southern Ocean winds increased by a factor of 2 showing expansion of all three deepwater formation regions.

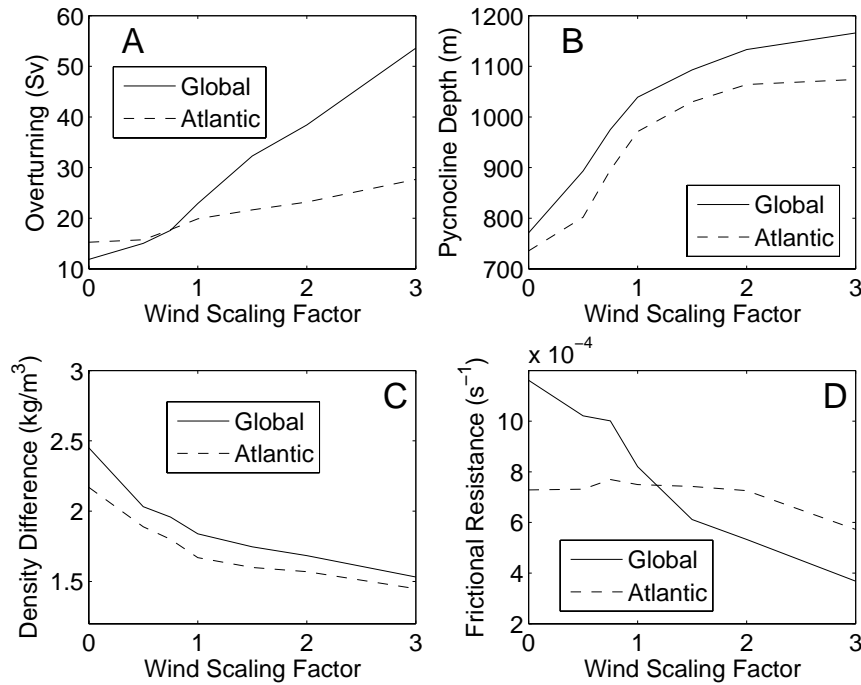


Figure 8: Response of the overturning circulation in a coupled ocean-sea ice-energy moisture balance atmosphere model to changes in Southern Ocean winds. Solid lines show global values, dashed lines those computed for the Atlantic alone. (A) Overturning in Sv. (B) Pycnocline depth in m. (C) Density difference in kg/m^3 . (D) Frictional resistance factor $\epsilon = g'D^2/M_n$.

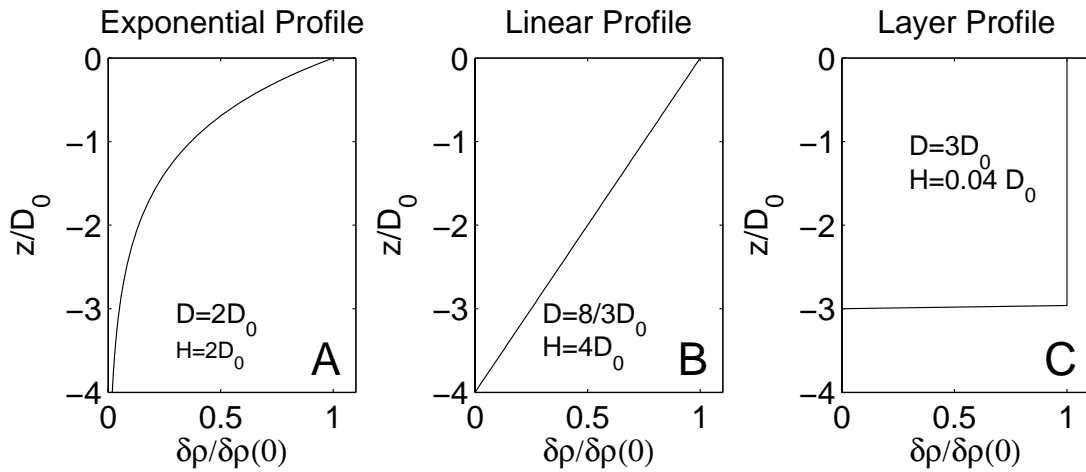


Figure 9. Schematic of three profiles of density anomaly normalized by the surface anomaly and the associated values of pycnocline depth (D , eqn 1) and pycnocline thickness (H , eqn. 6) associated with them.

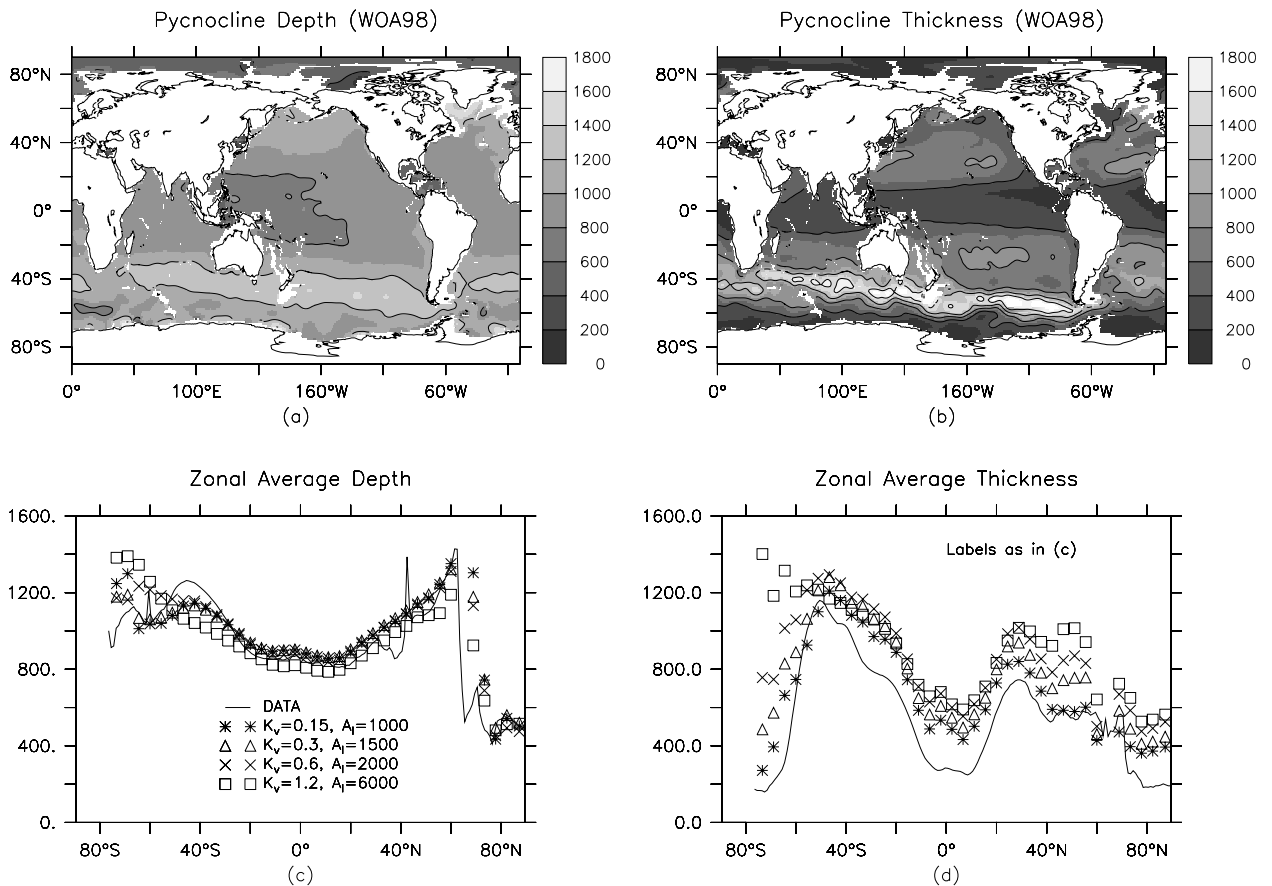


Figure 10: Pycnocline depth and thickness. (a) Pycnocline depth from the 1998 World Ocean Atlas. (b) Pycnocline thickness for the 1998 World Ocean Atlas. (c) Zonally averaged pycnocline depth compared with four “compensated” ocean-only models in which horizontal and vertical diffusion are varied together following G99. Note that the lines track each other, and the data, closely. (d.) Zonally averaged pycnocline thickness for the same set of models as in c. Note that there is now more variation, with more diffusive models having a notably thicker pycnocline.